

Weak Lensing of the CMB: Power Spectrum Covariance

Asantha Cooray*

Theoretical Astrophysics, California Institute of Technology, Pasadena, California 91125

E-mail: asante@tapir.caltech.edu

(To be submitted to Phys. Rev. D. — October 2001)

We discuss the non-Gaussian contribution to the power spectrum covariance of cosmic microwave background (CMB) anisotropies resulting through weak gravitational lensing angular deflections and the correlation of deflections with secondary sources of temperature fluctuations generated by the large scale structure, such as the integrated Sachs-Wolfe effect and the Sunyave-Zel'dovich effect. This additional contribution to the covariance of binned angular power spectrum, beyond the well known cosmic variance and any associated instrumental noise, results from a trispectrum, or a four point correlation function, in temperature anisotropy data. With substantially wide bins in multipole space, the resulting non-Gaussian contribution from lensing to the binned power spectrum variance is insignificant out to multipoles of a few thousand and is not likely to affect the cosmological parameter estimation with acoustic peaks and the damping tail. The non-Gaussian contribution to covariance, however, should be considered when interpreting binned CMB power spectrum measurements at multipoles of a few thousand corresponding to angular scales of few arcminutes and less.

I. INTRODUCTION

The applications of cosmic microwave background (CMB) anisotropy measurements are well known [1]; its ability to constrain most, or certain combinations of, parameters that define the currently favorable cold dark matter cosmologies with a cosmological constant has driven a wide number of experiments from ground and space. The advent of high sensitivity CMB anisotropy experiments with increasing capabilities to detect fluctuations over a wide range of scales now suggest the possibility that anisotropy power spectrum at small angular scales will soon be measured. At angular scales corresponding to few arcminutes and below, fluctuations are mostly dominated by secondary effects due to local large scale structure (LSS) between us and the recombination. Additionally, important non-linear second order effects such as the weak gravitational lensing of CMB leaves important imprints that can in return be used as a probe of cosmology or astrophysics related to evolution and growth of structures.

The increase in sensitivity of current and upcoming CMB experiments also suggest the possibility that non-Gaussian signals in the CMB temperature fluctuations may be detected and studied in detail. The deviations from Gaussianity in CMB temperature fluctuations arise through two scenarios: the existence of a primordial non-Gaussianity associated with initial fluctuations and the creation of non-Gaussian signals through non-linear mode-coupling effects related to secondary contributions. In currently favored cosmologies with adiabatic initial conditions, the primordial non-Gaussianity is non-existent or insignificant [2]. This leaves the secondary contributions, such as the Sunyave-Zel'dovich effect [3] due to inverse-Compton scattering of CMB photons via hot electrons, as the main source of non-Gaussianity. The existence of non-Gaussian fluctuations in temperature can be directly measured through higher order correla-

tions, such as a three-point function or a bispectrum in Fourier space [4,5]. The detection of non-Gaussianities at the three-point level can be optimized through the use of special statistics and matched filters [6] and through certain physical aspects associated with secondary effects, such as frequency dependence [7].

An additional effect due to non-Gaussianity include a contribution to the four-point correlation function, or a trispectrum in Fourier space, of CMB temperature fluctuations [8,9]. The four point correlations are of special interest since they quantify the sample variance and covariance of two point correlation or power spectrum measurements [10,11]. Thus, to properly understand the statistical measurements of CMB anisotropy fluctuations at the two point level, a proper understanding of the four point contributions is needed. Similarly, studies of the ability of CMB power spectrum measurements to constrain cosmology have been based on a Gaussian approximation to the sample variance and the assumption that covariance is negligible. If there are significant non-Gaussian contributions from the four point level that contribute to the power spectrum covariance, then it could affect the conversion of power spectrum measurements to estimates on cosmological parameters. Given the high precision level of cosmological parameter measurements expected from CMB, a careful consideration must be attached to understanding the presence of non-Gaussian signals at the four point level. Thus, the basic goal of this paper is to understand to what extent Gaussian assumption on CMB power spectrum covariance remains to hold when non-Gaussian contributions are included.

As discussed in previous studies (e.g., [4]), one of the most important non-linear contribution to CMB temperature fluctuations is weak gravitational lensing. Similar to the weak lensing contribution to CMB anisotropy at the three-point level, the contributions to the four point level results from the non-linear mode-coupling nature of weak lensing effect and the correlation between

weak lensing angular deflections and secondary effects that trace the same large scale structure. The trispectrum due to lensing alone is studied in [9] and the same trispectrum, under an all-sky formulation, is also considered in [8]. Here, we focus on the contribution of the trispectrum to the power spectrum covariance which was not considered in previous works. We also include the trispectrum resulting from the correlation between lensing and secondary effects such as the integrated Sachs-Wolfe (ISW; [12]) effect and the thermal SZ [3] effect. The latter effect has now been imaged towards massive galaxy clusters where the temperature of the scattering medium can be as high as 10 keV producing temperature fluctuations of order 1 mK [13].

In general, we do not expect secondary contributions such as the thermal SZ effect to be an important non-Gaussian contribution to temperature fluctuations, since its signal can be easily separated from the thermal CMB spectrum based on multifrequency information [7]. Still, we consider its correlation with lensing as a source of covariance as certain experiments, especially at small angular scales, may not have the adequate frequency coverage for a proper separation. In a previous paper, we discussed the non-Gaussian covariance resulting from SZ alone is discussed in [14], where we also considered the effect of full-covariance, compared to Gaussian variance assumption, on the estimation of parameters related to the SZ effect. As discussed there, due to highly non-Gaussian behavior of the SZ signal resulting from its dependence on massive halos such as galaxy clusters, the determination of parameters that define the SZ contribution is affected by the presence of non-Gaussian contribution to the covariance.

In §III, we introduce the basic ingredients for the present calculation. The CMB anisotropy trispectra due to weak lensing and correlations between weak lensing and secondary effects are derived in §III. In §IV, we calculate the CMB power spectrum covariance due to weak lensing and discuss our results in §V. In §VI we conclude with a summary.

II. GENERAL DERIVATION

Large-scale structure between us and the last scattering surface deflects CMB photons propagating towards us. Since lensing effect on CMB is essentially a distribution of photons, from large scales to small scales, the resulting effect appears only in the second order [8]. In weak gravitational lensing, the deflection angle on the sky given by the angular gradient of the lensing potential, $\delta(\hat{\mathbf{n}}) = \nabla\phi(\hat{\mathbf{n}})$, which is itself a projection of the gravitational potential, Φ (see e.g. [15]),

$$\phi(\hat{\mathbf{m}}) = -2 \int_0^{r_0} dr \frac{d_A(r_0 - r)}{d_A(r)d_A(r_0)} \Phi(r, \hat{\mathbf{m}}r). \quad (1)$$

The quantities here are the conformal distance or look-back time, from the observer, given by

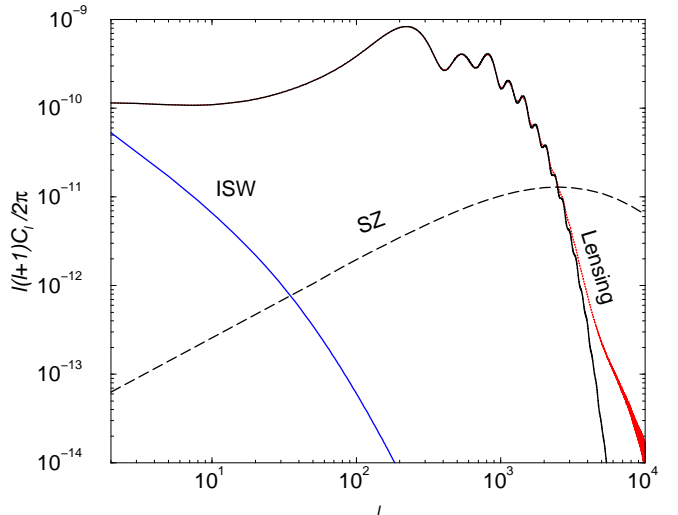


FIG. 1. Power spectrum of the CMB temperature anisotropies in the fiducial Λ CDM model. We have also shown the weak lensing, integrated Sachs-Wolfe and the SZ secondary contributions to angular power spectrum.

$$r(z) = \int_0^z \frac{dz'}{H(z')}, \quad (2)$$

and the analogous angular diameter distance

$$d_A = H_0^{-1} \Omega_K^{-1/2} \sinh(H_0 \Omega_K^{1/2} r), \quad (3)$$

with the expansion rate for adiabatic CDM cosmological models with a cosmological constant given by

$$H^2 = H_0^2 [\Omega_m(1+z)^3 + \Omega_K(1+z)^2 + \Omega_\Lambda]. \quad (4)$$

Here, H_0 can be written as the inverse Hubble distance today $H_0^{-1} = 2997.9h^{-1}\text{Mpc}$. We follow the conventions that in units of the critical density $3H_0^2/8\pi G$, the contribution of each component is denoted Ω_i , $i = c$ for the CDM, b for the baryons, Λ for the cosmological constant. We also define the auxiliary quantities $\Omega_m = \Omega_c + \Omega_b$ and $\Omega_K = 1 - \sum_i \Omega_i$, which represent the matter density and the contribution of spatial curvature to the expansion rate respectively. Note that as $\Omega_K \rightarrow 0$, $d_A \rightarrow r$ and we define $r(z = \infty) = r_0$. Though we present a general derivation of the trispectrum contribution to the covariance, we show results for the currently favorable Λ CDM cosmology with $\Omega_b = 0.05$, $\Omega_m = 0.35$, $\Omega_\Lambda = 0.65$ and $h = 0.65$.

The lensing potential in equation 1 can be related to the well known convergence generally encountered in conventional lensing studies involving galaxy shear [15]

$$\begin{aligned} \kappa(\hat{\mathbf{m}}) &= \frac{1}{2} \nabla^2 \phi(\hat{\mathbf{m}}) \\ &= - \int_0^{r_0} dr \frac{d_A(r)d_A(r_0 - r)}{d_A(r_0)} \nabla_\perp^2 \Phi(r, \hat{\mathbf{m}}r), \end{aligned} \quad (5)$$

where note that the 2D Laplacian operating on Φ is a spatial and not an angular Laplacian. Though the two

terms κ and ϕ contain differences with respect to radial and wavenumber weights, these differences cancel with the Limber approximation [16]. The spherical harmonic moments of these two quantities are simply proportional with multiplicative factors in l

$$\begin{aligned}\phi_{lm} &= -\frac{2}{l(l+1)}\kappa_{lm} = \int d\hat{\mathbf{n}} Y_l^{m*}(\hat{\mathbf{n}})\phi(\hat{\mathbf{n}}) \\ &= i^l \int \frac{d^3\mathbf{k}}{2\pi^2} \delta(\mathbf{k}) Y_l^{m*}(\hat{\mathbf{k}}) I_l^{\text{len}}(k),\end{aligned}\quad (6)$$

where

$$\begin{aligned}I_l^{\text{len}}(k) &= \int_0^{r_0} dr W^{\text{len}}(k, r) j_l(kr), \\ W^{\text{len}}(k, r) &= -3\Omega_m \left(\frac{H_0}{k}\right)^2 F(r) \frac{d_A(r_0 - r)}{d_A(r)d_A(r_0)}.\end{aligned}\quad (7)$$

Here, we have used the Rayleigh expansion of a plane wave

$$e^{i\mathbf{k}\cdot\hat{\mathbf{n}}r} = 4\pi \sum_{lm} i^l j_l(kr) Y_l^{m*}(\hat{\mathbf{k}}) Y_l^m(\hat{\mathbf{n}}),\quad (8)$$

and the fact that $\nabla^2 Y_l^m = -l(l+1)Y_l^m$.

Note that the cosmological Poisson equation relates fluctuations in the density field, given by δ in equation 6, to the fluctuations in the gravitational potential, Φ :

$$\Phi = \frac{3}{2}\Omega_m \left(\frac{H_0}{k}\right)^2 \left(1 + 3\frac{H_0^2}{k^2}\Omega_K\right)^{-2} \frac{G(r)}{a} \delta(k, 0),\quad (9)$$

with the growth function, $\delta(k, r) = G(r)\delta(k, 0)$ [17], given by

$$G(r) \propto \frac{H(r)}{H_0} \int_{z(r)}^{\infty} dz' (1+z') \left(\frac{H_0}{H(z')}\right)^3.\quad (10)$$

Note that in the matter dominated epoch $G \propto a = (1+z)^{-1}$.

Expanding the lensing potential to multiple moments,

$$\phi(\hat{\mathbf{n}}) = \sum \phi_{lm} Y_l^m(\hat{\mathbf{n}}),\quad (11)$$

we can write its correlation function

$$\langle \phi(\hat{\mathbf{n}})\phi(\hat{\mathbf{m}}) \rangle = \sum \langle \phi_{lm}^* \phi_{l'm'} \rangle Y_l^{m*}(\hat{\mathbf{n}}) Y_{l'}^{m'}(\hat{\mathbf{m}}).\quad (12)$$

The power spectrum of lensing potentials is now given through

$$\langle \phi_{lm}^* \phi_{lm} \rangle = \delta_{ll'} \delta_{mm'} C_l^{\phi\phi}\quad (13)$$

as

$$C_l^{\phi\phi} = \frac{2}{\pi} \int k^2 dk P(k) I_l^{\text{len}}(k) I_l^{\text{len}}(k).\quad (14)$$

Here, we have introduced the power spectrum of density fluctuations

$$\langle \delta(\mathbf{k})\delta(\mathbf{k}') \rangle = (2\pi)^3 \delta^D(\mathbf{k} + \mathbf{k}') P(k),\quad (15)$$

where δ^D is the Dirac delta function and

$$\frac{k^3 P(k)}{2\pi^2} = \delta_H^2 \left(\frac{k}{H_0}\right)^{n+3} T^2(k),\quad (16)$$

in linear perturbation theory. We use the fitting formulae of [18] in evaluating the transfer function $T(k)$ for CDM models. Here, δ_H is the amplitude of present-day density fluctuations at the Hubble scale; with $n = 1$, we adopt the COBE normalization for δ_H [19] of 4.2×10^{-5} , consistent with galaxy cluster abundance [20], with $\sigma_8 = 0.86$.

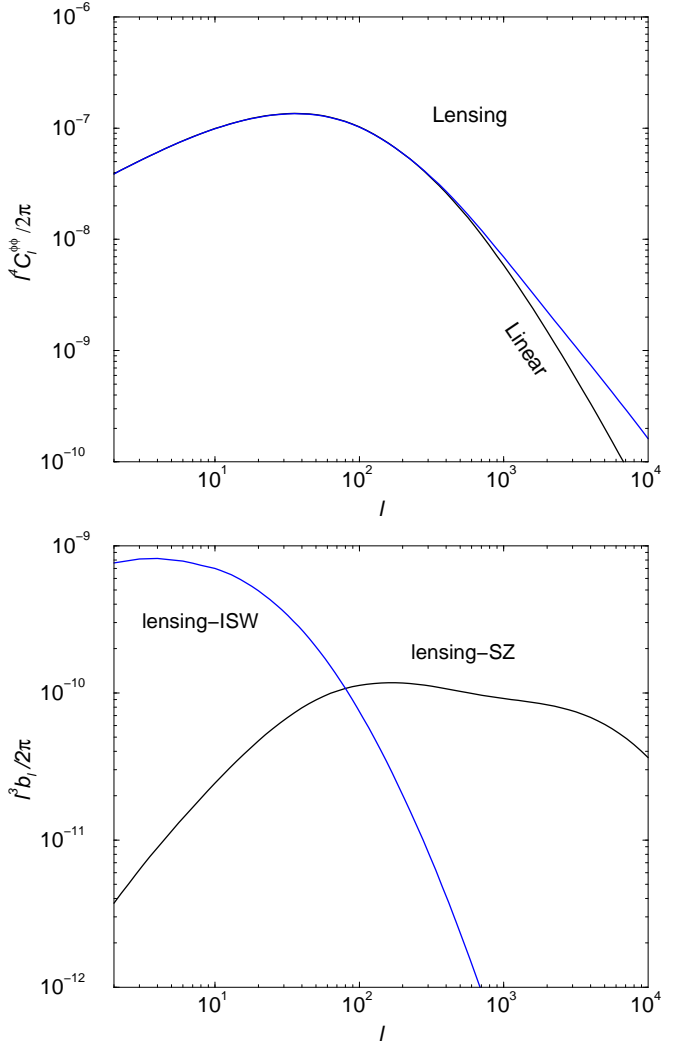


FIG. 2. Power spectra (a) of lensing angular deflections and (b) lensing-isw and lensing-sz cross-correlation. In (a), we show the lensing deflection power spectrum under linear perturbation theory description of the matter fluctuations and using the halo model. As shown, the lensing deflection power peaks at multipoles of ~ 40 and act as an effective window function which smooths the CMB power spectrum. In (b), the lensing-SZ correlation is calculated with the halo approach while lensing-ISW correlation follows the use of linear theory dark matter power spectrum.

Note that an expression of the type in equation (14) can be evaluated efficiently with a version of the Limber approximation [16], called the weak coupling approximation [21], such that

$$\begin{aligned} I_l^X(k) &\equiv \int_0^{r_0} dr W^X(k, r) j_l(kr) \\ &\approx W^X(k, l/k) \int_0^\infty dr j_l(kr) \quad (k \frac{W}{\dot{W}} \gg 1) \\ &= W^X(k, l/k) \frac{\sqrt{\pi}}{2k} \frac{\Gamma[(l+1)/2]}{\Gamma[(l+2)/2]}. \end{aligned} \quad (17)$$

For $l \gg 1$, the ratio of gamma functions goes to $\sqrt{2/l}$ simplifying further. Using a change of variables such that $d_A = l/k$, we obtain an approximation for the power spectrum of lensing potentials as

$$\begin{aligned} C_l^{\phi\phi} &= \frac{2}{\pi} \int k^2 dk P(k) I_l^{\text{len}}(k) I_l^{\text{len}}(k) \\ &\approx \int_0^{r_0} \frac{dr}{d_A^2} \left[W^{\text{len}}\left(\frac{l}{d_A}, r\right) \right]^2 P\left(\frac{l}{d_A}\right). \end{aligned} \quad (18)$$

Since the same large scale structure responsible for deflections in CMB photons produce contributions to the anisotropies through other effects, there is a correlation between the deflection potential and secondary sources of temperature fluctuations. As in the power spectrum of deflection potential, using statistical isotropy, we write the correlation as

$$\begin{aligned} \langle \phi_{lm}^* a_{lm}^S \rangle &\equiv b_l^S \equiv \frac{-2}{l(l+1)} C_l^{T\kappa}, \\ &= \frac{2}{\pi} \int k^2 dk P(k) I_l^S(k) I_l^{\text{len}}(k), \\ &\approx \int_0^{r_0} \frac{dr}{d_A^2} W^S\left(\frac{l}{d_A}, r\right) W^{\text{len}}\left(\frac{l}{d_A}, r\right) P\left(\frac{l}{d_A}\right). \end{aligned} \quad (19)$$

Here,

$$T^S(\hat{\mathbf{n}}) = \sum a_{lm}^S Y_l^m(\hat{\mathbf{n}}), \quad (20)$$

and we have used equation (6) to relate the power spectrum b_l^S of Refs. [4,5] and the κ -secondary cross power spectrum of Ref. [22]. The last line represents the Limber approximation and we have assumed that the secondary anisotropies are related to the first order fluctuations in the density field projected along the line of sight,

$$\begin{aligned} a_{lm}^S &= i^l \int \frac{d^3 \mathbf{k}}{2\pi^2} \delta(\mathbf{k}) I_l^S(k) Y_l^m(\hat{\mathbf{k}}), \\ I_l^S(k) &= \int dr W^S(k, r) j_l(kr). \end{aligned} \quad (21)$$

In the present paper we consider two secondary effects that correlate with lensing deflections: integrated Sachs-Wolfe (ISW) effect and the Sunyaev-Zel'dovich (SZ) effect. Since higher order effects such as the kinetic SZ

effect, due to the line of sight motion of electrons, is second order in density fluctuations, there is no first order cross-correlation with the lensing potentials. The ISW [12] effect results from the late time decay of gravitational potential fluctuations. The resulting temperature fluctuations in the CMB can be written as

$$T^{\text{ISW}}(\hat{\mathbf{n}}) = -2 \int_0^{r_0} dr \dot{\Phi}(r, \hat{\mathbf{n}} r). \quad (22)$$

The weight function associated with the ISW effect is given by

$$W^{\text{ISW}}(k) = -3\Omega_m \left(\frac{H_0}{k}\right)^2 \dot{F}(r), \quad (23)$$

which can be used to calculate the correlation between lensing potential and the ISW effect through equation 19.

The SZ effect leads to an effective temperature fluctuation in the CMB given by the integrated pressure fluctuation along the line of sight:

$$T^{\text{SZ}}(\hat{\mathbf{n}}) = g(x) \int dr a(r) \frac{k_B \sigma_T}{m_e c^2} n_e(r) T_e(r) \quad (24)$$

where σ_T is the Thomson cross-section, n_e is the electron number density, r is the comoving distance, and $g(x) = x \coth(x/2) - 4$ with $x = h\nu/k_B T_{\text{CMB}}$ is the spectral shape of SZ effect. At Rayleigh-Jeans (RJ) part of the CMB, $g(x) = -2$. For the rest of this paper, we assume observations in the Rayleigh-Jeans regime of the spectrum; an experiment such as Planck with sensitivity beyond the peak of the spectrum can separate out SZ contributions based on the spectral signature, $g(x)$ [7].

For the correlation between lensing and SZ effect, we follow the halo model approach of [23] (see [24] for further details) which allows a semi-analytical approach to calculate the power spectrum of large scale structure pressure fluctuations. At RJ part of the frequency spectrum, the SZ weight function is

$$W^{\text{SZ}}(r) = -2 \frac{k_B \sigma_T \bar{n}_e}{a(r)^2 m_e c^2} \quad (25)$$

where \bar{n}_e is the mean electron density today. With the halo model, we replace the clustering of dark matter with that of pressure when describing the SZ effect. The cross-correlation between lensing and SZ then involves the cross-power spectrum between pressure and dark matter.

In figure 1, we show the angular power spectrum of CMB anisotropies [25] with secondary contributions through weak lensing, ISW and SZ effects. The SZ angular power spectrum was calculated using the halo approach of [23]. The lensing angular deflection power spectrum and the resulting correlation power spectra between lensing and ISW, and, lensing and SZ effects are shown in figure 2.

III. LENSING CONTRIBUTION TO CMB

In order to derive weak lensing contributions to the CMB trispectrum, we follow Hu [8] and Zaldarriaga [9]. We formulate the contribution under a flat sky approximation; this formulation is adequate given that we are mostly interested in non-Gaussian effects due to lensing at small angular scales corresponding to multipoles $\gtrsim 1000$. In general, the flat-sky approach simplifies the derivation and computation through the replacement of mode-coupling Wigner symbols through angles.

As discussed in prior papers [4,5,8], weak lensing maps temperature through the angular deflections resulting along the photon path by

$$\begin{aligned}\Theta^t(\hat{\mathbf{n}}) &= \Theta(\hat{\mathbf{n}} + \nabla\phi) \\ &= \Theta(\hat{\mathbf{n}}) + \nabla_i\phi(\hat{\mathbf{n}})\nabla^i\Theta(\hat{\mathbf{n}}) \\ &\quad + \frac{1}{2}\nabla_i\phi(\hat{\mathbf{n}})\nabla_j\phi(\hat{\mathbf{n}})\nabla^i\nabla^j\Theta(\hat{\mathbf{n}}) + \dots\end{aligned}\quad (26)$$

As expected for lensing, note that the remapping conserves the surface brightness distribution of CMB. Here, $\Theta(\hat{\mathbf{n}})$ is the unlensed primary component of CMB and $\Theta^t(\hat{\mathbf{n}})$ is the total contribution. It should be understood that in the presence of low redshift contributions to CMB resulting through large scale structure, the total contribution includes a secondary contribution which we denote by $\Theta^s(\hat{\mathbf{n}})$. Since weak lensing deflection angles also trace the large scale structure at low redshifts, secondary effects which are first order in density or potential fluctuations also correlate with the lensing deflection angle ϕ .

Taking the Fourier transform, as appropriate for a flat-sky, we write

$$\begin{aligned}\tilde{\Theta}(\mathbf{l}_1) &= \int d\hat{\mathbf{n}} \tilde{\Theta}(\hat{\mathbf{n}}) e^{-i\mathbf{l}_1 \cdot \hat{\mathbf{n}}} \\ &= \Theta(\mathbf{l}_1) - \int \frac{d^2\mathbf{l}_1'}{(2\pi)^2} \Theta(\mathbf{l}_1') L(\mathbf{l}_1, \mathbf{l}_1'),\end{aligned}\quad (27)$$

where

$$\begin{aligned}L(\mathbf{l}_1, \mathbf{l}_1') &= \phi(\mathbf{l}_1 - \mathbf{l}_1') (\mathbf{l}_1 - \mathbf{l}_1') \cdot \mathbf{l}_1' + \frac{1}{2} \int \frac{d^2\mathbf{l}_1''}{(2\pi)^2} \phi(\mathbf{l}_1'') \\ &\quad \times \phi^*(\mathbf{l}_1'' + \mathbf{l}_1' - \mathbf{l}_1) (\mathbf{l}_1'' \cdot \mathbf{l}_1') (\mathbf{l}_1'' + \mathbf{l}_1' - \mathbf{l}_1) \cdot \mathbf{l}_1'\end{aligned}$$

We define the power spectrum and the trispectrum in the flat sky approximation following the usual way

$$\begin{aligned}\langle \Theta^t(\mathbf{l}_1) \Theta^t(\mathbf{l}_2) \rangle &= (2\pi)^2 \delta_D(\mathbf{l}_{12}) \tilde{C}_l^\Theta, \\ \langle \Theta^t(\mathbf{l}_1) \dots \Theta^t(\mathbf{l}_4) \rangle_c &= (2\pi)^2 \delta_D(\mathbf{l}_{1234}) \tilde{T}^\Theta(\mathbf{l}_1, \mathbf{l}_2, \mathbf{l}_3, \mathbf{l}_4).\end{aligned}\quad (29)$$

A. Power spectrum

The power spectrum, according to the present formulation, is discussed in [8] and we can write

$$\begin{aligned}\tilde{C}_l^\Theta &= \left[1 - \int \frac{d^2\mathbf{l}_1}{(2\pi)^2} C_{l_1}^{\phi\phi} (\mathbf{l}_1 \cdot \mathbf{l})^2 \right] C_l^\Theta \\ &\quad + \int \frac{d^2\mathbf{l}_1}{(2\pi)^2} C_{|\mathbf{l}-\mathbf{l}_1|}^\Theta C_{l_1}^{\phi\phi} [(\mathbf{l} - \mathbf{l}_1) \cdot \mathbf{l}_1]^2.\end{aligned}\quad (30)$$

As written, the second term shows the smoothing behavior of weak lensing through a convolution (eqn. 30) of the CMB power spectrum (see discussion in [8]). With respect to lensing contribution, there are two limiting cases: when $\mathbf{l} - \mathbf{l}_1 \approx \mathbf{l}$ and cmb power is constant, one can take the CMB power spectrum out of the integral in the second term such that

$$\begin{aligned}\tilde{C}_l^\Theta &\approx \left[1 - \int \frac{d^2\mathbf{l}_1}{(2\pi)^2} C_{l_1}^{\phi\phi} (\mathbf{l}_1 \cdot \mathbf{l})^2 \right] C_l^\Theta \\ &\quad + C_l^\Theta \int \frac{d^2\mathbf{l}_1}{(2\pi)^2} C_{l_1}^{\phi\phi} (\mathbf{l} \cdot \mathbf{l}_1)^2.\end{aligned}\quad (31)$$

Thus, there is a net cancellation of terms involving lensing potential power spectrum and $\tilde{C}_l^\Theta \approx C_l^\Theta$ producing the well known result that lensing shifts but does not create power on large scales [8]. On small scales where there is no or little intrinsic power in the CMB, the second term behaves such that

$$\tilde{C}_l^\Theta \approx \frac{1}{2} l^2 C_l^{\phi\phi} \int \frac{d^2\mathbf{l}_1}{(2\pi)^2} l_1^2 C_{l_1}^\Theta. \quad (32)$$

Here, the power generated is effectively the lensing of the temperature gradient associated with the damping tail of CMB anisotropy power spectrum. This small angular scale limit and its uses as a probe of large scale structure density power spectrum and mass distribution of collapsed halos such as galaxy clusters is considered in [27].

B. Trispectrum

The calculation of the trispectrum follows similar to the power spectrum. Here, we explicitly show the calculation for one term of the trispectrum and add all other terms through permutations. First we consider the cumulants involving four temperature terms in Fourier space:

$$\begin{aligned}\langle \Theta^t(\mathbf{l}_1) \dots \Theta^t(\mathbf{l}_4) \rangle_c &= \\ &\left\langle \left(\Theta(\mathbf{l}_1) - \int \frac{d^2\mathbf{l}_1'}{(2\pi)^2} \Theta(\mathbf{l}_1') L(\mathbf{l}_1, \mathbf{l}_1') \right) \right. \\ &\quad \times \left. \left(\Theta(\mathbf{l}_2) - \int \frac{d^2\mathbf{l}_2'}{(2\pi)^2} \Theta(\mathbf{l}_2') L(\mathbf{l}_2, \mathbf{l}_2') \right) \Theta(\mathbf{l}_3) \Theta(\mathbf{l}_4) \right\rangle \\ &= \left\langle \int \frac{d^2\mathbf{l}_1'}{(2\pi)^2} \Theta(\mathbf{l}_1') L(\mathbf{l}_1, \mathbf{l}_1') \int \frac{d^2\mathbf{l}_2'}{(2\pi)^2} \Theta(\mathbf{l}_2') L(\mathbf{l}_2, \mathbf{l}_2') \right. \\ &\quad \times \left. \Theta(\mathbf{l}_3) \Theta(\mathbf{l}_4) \right\rangle.\end{aligned}\quad (33)$$

As written, to the lowest order, we find that contributions come from the first order term in L given in equation (29). We further simplify to obtain

$$\begin{aligned}
\langle \Theta^t(l_1) \dots \Theta^t(l_4) \rangle_c &= \\
&= \left\langle \int \frac{d^2 l'_1}{(2\pi)^2} \Theta(l_1') \phi(l_1 - l_1') (l_1 - l_1') \cdot l_1' \right. \\
&\quad \times \int \frac{d^2 l'_2}{(2\pi)^2} \Theta(l_2') \phi(l_2 - l_2') (l_2 - l_2') \cdot l_2' \Theta(l_3) \Theta(l_4) \left. \right\rangle \\
&= C_{l_3}^\Theta C_{l_4}^\Theta \left\langle \phi(l_1 + l_3) \phi(l_2 + l_4) \right\rangle (l_1 + l_3) \cdot l_3 (l_2 + l_4) \cdot l_4 \\
&\quad + \text{Perm.}, \tag{34}
\end{aligned}$$

where there is an additional term through a permutation involving the interchange of $l_1 + l_3$ with $l_1 + l_4$. Introducing the power spectrum of lensing potentials, we further simplify to obtain the CMB trispectrum due to gravitational lensing:

$$\begin{aligned}
\tilde{T}^\Theta(l_1, l_2, l_3, l_4) &= -C_{l_3}^\Theta C_{l_4}^\Theta \left[C_{|l_1+l_3|}^{\phi\phi} (l_1 + l_3) \cdot l_3 (l_1 + l_3) \cdot l_4 \right. \\
&\quad \left. + C_{|l_2+l_3|}^{\phi\phi} (l_2 + l_3) \cdot l_3 (l_2 + l_3) \cdot l_4 \right] + \text{Perm.}, \tag{35}
\end{aligned}$$

where the permutations now contain 5 additional terms with the replacement of (l_3, l_4) pair by other combination of pairs.

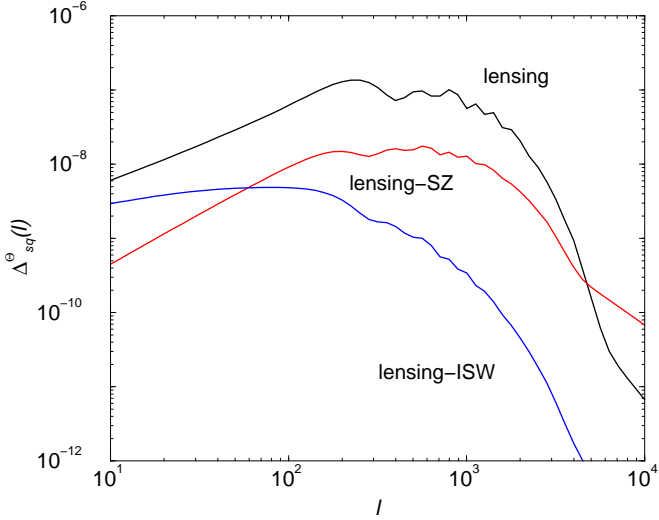


FIG. 3. CMB anisotropy trispectrum resulting from lensing, lensing-ISW and lensing-SZ correlations. The lensing trispectrum generally follows the shape of the CMB power spectrum while lensing-ISW and lensing-SZ trispectra depicts the behavior of correlation power between lensing and these secondary effects.

The non-Gaussian contribution to the trispectrum, through coupling of lensing deflection angle to secondary effects, can be calculated with the replacement of $\Theta(l_3)$ and $\Theta(l_4)$ in equation (33) by $\Theta^s(l_3)$ and $\Theta^s(l_4)$ containing the sources of secondary fluctuations. Thus, we can no longer consider cumulants such as $\langle \Theta(l_1') \Theta^s(l_3) \rangle$ as

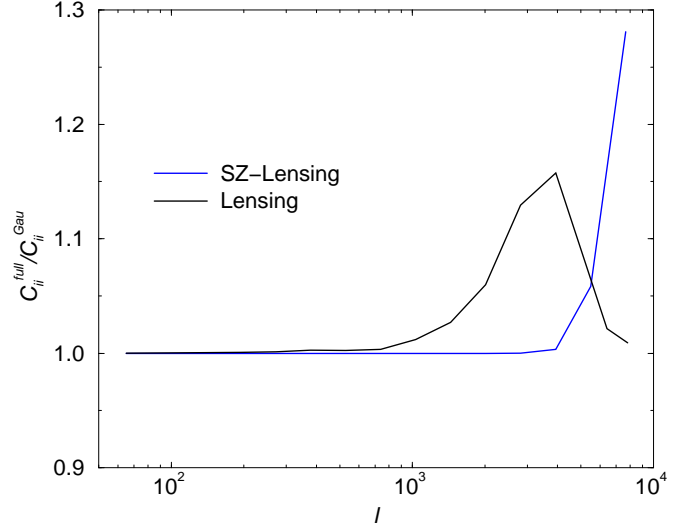


FIG. 4. The ratio of full variance, including non-Gaussian covariance, to that when non-Gaussian trispectrum contributions are neglected. This ratio shows the fractional change in the variance, or the errors along the diagonal of the covariance matrix. Out of multipoles of a few thousand, the increase due to lensing is less than few percent and at the smallest scale there is no change from the lensing alone trispectrum as its contributions are substantially small. The lensing-SZ trispectrum only makes noticeable contributions at the smallest scale. The resulting changes from the lensing-ISW trispectrum is below 10^{-6} and can be ignored.

the secondary effects are decoupled from recombination where primary fluctuations are imprinted. However, contributions come from the correlation between Θ^s and the lensing deflection ϕ . Here, contributions of equal importance come from both the first and second order terms in L written in equation (29). First, we note

$$\begin{aligned}
\langle \Theta(l_1) \dots \Theta(l_4) \rangle_c &= \\
&\quad \left\langle \left(\Theta(l_1) - \int \frac{d^2 l'_1}{(2\pi)^2} \Theta(l_1') L(l_1, l_1') \right) \right. \\
&\quad \times \left. \left(\Theta(l_2) - \int \frac{d^2 l'_2}{(2\pi)^2} \Theta(l_2') L(l_2, l_2') \right) \Theta^s(l_3) \Theta^s(l_4) \right\rangle \\
&= -C_{l_1} \langle L(l_2, -l_1) \Theta^s(l_3) \Theta^s(l_4) \rangle \\
&\quad - C_{l_2} \langle L(l_1, -l_2) \Theta^s(l_3) \Theta^s(l_4) \rangle \\
&\quad + \int \frac{d^2 l'_1}{(2\pi)^2} C_{l'_1} \langle L(l_2, -l_1') L(l_1, l_1') \Theta^s(l_3) \Theta^s(l_4) \rangle \tag{36}
\end{aligned}$$

Contributions to the trispectrum from the first two terms come through the second order term in L , with the two ϕ terms coupling to Θ^s . In the last term, contributions come from the first order term of L similar to the lensing alone contribution to trispectrum.

After some straightforward simplifications, we write the connected part of the trispectrum involving lensing-secondary coupling as

$$\begin{aligned}
\tilde{T}^\Theta(\mathbf{l}_1, \mathbf{l}_2, \mathbf{l}_3, \mathbf{l}_4) = & \\
- C_{l_3}^{\phi s} C_{l_4}^{\phi s} & \left[C_{l_1}^\Theta (\mathbf{l}_3 \cdot \mathbf{l}_1) (\mathbf{l}_4 \cdot \mathbf{l}_1) + C_{l_2}^\Theta (\mathbf{l}_3 \cdot \mathbf{l}_2) (\mathbf{l}_4 \cdot \mathbf{l}_2) \right. \\
+ \mathbf{l}_3 \cdot (\mathbf{l}_1 + \mathbf{l}_3) \mathbf{l}_4 \cdot (\mathbf{l}_2 + \mathbf{l}_4) C_{l_1 l_3}^\Theta + \mathbf{l}_4 \cdot (\mathbf{l}_1 + \mathbf{l}_4) \mathbf{l}_3 \cdot (\mathbf{l}_2 + \mathbf{l}_3) C_{l_1 l_4}^\Theta \\
+ \text{Perm.} .
\end{aligned}$$

Note that the first two terms come from the first and second term in equation (36), while the last two terms in above are from the third term. As before, through permutations, there are five additional terms involving the pairings of (l_3, l_4) .

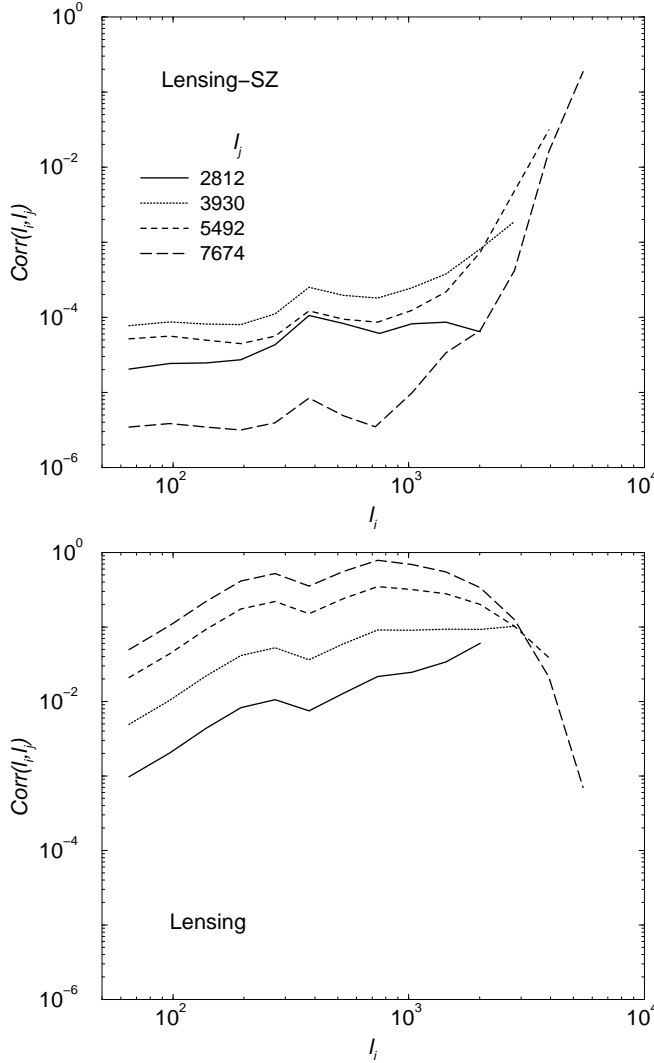


FIG. 5. The correlation coefficients of (a) lensing and (b) lensing-SZ contributions to the covariance of the CMB angular power spectrum. In the case of lensing, the correlations shows the general behavior of lensing effects on CMB where power is transferred from large angular scales with acoustic peaks to small angular scales, thereby correlating small and large angular scales at the tens of percent level or more. For experiments, such as Planck, that will measure the power spectrum to multipoles of ~ 2000 , the resulting correlations between bins are less than a percent.

IV. POWER SPECTRUM COVARIANCE

For the purpose of this calculation, we assume that CMB power spectrum will measure binned logarithmic band powers at several l_i 's in multipole space with bins (37) of thickness δl_i .

$$c_i = \int_{si} \frac{d^2 l}{A_{si}} \frac{l^2}{2\pi} \Theta(\mathbf{l}) \Theta(-\mathbf{l}), \quad (38)$$

where $A_s(l_i) = \int d^2 l$ is the area of 2D shell in multipole and can be written as $A_s(l_i) = 2\pi l_i \delta l_i + \pi(\delta l_i)^2$.

We can now write the signal covariance matrix as

$$C_{ij} = \frac{1}{A} \left[\frac{(2\pi)^2}{A_{si}} 2C_i^2 + T_{ij}^\Theta \right], \quad (39)$$

$$T_{ij}^\Theta = \int \frac{d^2 l_i}{A_{si}} \int \frac{d^2 l_j}{A_{sj}} \frac{l_i^2 l_j^2}{(2\pi)^2} T^\Theta(\mathbf{l}_i, -\mathbf{l}_i, \mathbf{l}_j, -\mathbf{l}_j), \quad (40)$$

where A is the area of the survey in steradians. Again the first term is the Gaussian contribution to the sample variance and includes, in addition to the primary component, contribution through lensing and secondary effects. The second term is the non-Gaussian contribution. A realistic survey will also include instrumental noise contributions and we can modify the Gaussian variance to include the noise through an additional noise contribution to the power spectrum

$$C_l^t = C_l^\Theta + N_l \quad (41)$$

where N_l is the power spectrum of detector and other sources of noise introduced by the experiment.

For the power spectrum covariance, we are interested in the case when $\mathbf{l}_2 = -\mathbf{l}_1$ with $|\mathbf{l}_1| = l_i$ and $\mathbf{l}_4 = -\mathbf{l}_3$ with $|\mathbf{l}_3| = l_j$. This denotes parallelograms for the trispectrum configuration in multipolar or Fourier space.

In the case of lensing contribution to the trispectrum, with the configuration required for the power spectrum covariance, we can write

$$\begin{aligned}
T^\Theta(\mathbf{l}_i, -\mathbf{l}_i, \mathbf{l}_j, -\mathbf{l}_j) = & \\
C_{l_i}^\Theta C_{l_i}^\Theta & \left[C_{|\mathbf{l}_i + \mathbf{l}_j|}^{\phi\phi} [(\mathbf{l}_i + \mathbf{l}_j) \cdot \mathbf{l}_i]^2 + C_{|\mathbf{l}_i - \mathbf{l}_j|}^{\phi\phi} [(\mathbf{l}_i - \mathbf{l}_j) \cdot \mathbf{l}_i]^2 \right] \\
+ C_{l_i}^\Theta C_{l_j}^\Theta & \left[C_{|\mathbf{l}_i + \mathbf{l}_j|}^{\phi\phi} [(\mathbf{l}_i + \mathbf{l}_j) \cdot \mathbf{l}_j]^2 + C_{|\mathbf{l}_i - \mathbf{l}_j|}^{\phi\phi} [(\mathbf{l}_i - \mathbf{l}_j) \cdot \mathbf{l}_j]^2 \right] \\
+ 2C_{l_i}^\Theta C_{l_j}^\Theta & \left[C_{|\mathbf{l}_i + \mathbf{l}_j|}^{\phi\phi} (\mathbf{l}_i + \mathbf{l}_j) \cdot \mathbf{l}_i (\mathbf{l}_i + \mathbf{l}_j) \cdot \mathbf{l}_j \right. \\
& \left. - C_{|\mathbf{l}_i - \mathbf{l}_j|}^{\phi\phi} (\mathbf{l}_i - \mathbf{l}_j) \cdot \mathbf{l}_i (\mathbf{l}_i - \mathbf{l}_j) \cdot \mathbf{l}_j \right], \quad (42)
\end{aligned}$$

and includes all terms with no additional permutations.

Similarly, for the lensing-secondary trispectrum we have

$$\begin{aligned}
T^\Theta(\mathbf{l}_i, -\mathbf{l}_i, \mathbf{l}_j, -\mathbf{l}_j) = & \\
2(\mathbf{l}_i \cdot \mathbf{l}_j)^2 & \left[\left(C_{l_i}^{\phi s} \right)^2 C_{l_j}^\Theta + \left(C_{l_j}^{\phi s} \right)^2 C_{l_i}^\Theta \right]
\end{aligned}$$

$$\begin{aligned}
& - \left[[\mathbf{l}_i \cdot (\mathbf{l}_i + \mathbf{l}_j)]^2 \left(C_{l_i}^{\phi s} \right)^2 + [\mathbf{l}_j \cdot (\mathbf{l}_i + \mathbf{l}_j)]^2 \left(C_{l_j}^{\phi s} \right)^2 \right] C_{|\mathbf{l}_i + \mathbf{l}_j|}^{\Theta} \\
& - \left[[\mathbf{l}_i \cdot (\mathbf{l}_i - \mathbf{l}_j)]^2 \left(C_{l_i}^{\phi s} \right)^2 + [\mathbf{l}_j \cdot (\mathbf{l}_i - \mathbf{l}_j)]^2 \left(C_{l_j}^{\phi s} \right)^2 \right] C_{|\mathbf{l}_i - \mathbf{l}_j|}^{\Theta} \\
& + 2 [\mathbf{l}_i \cdot (\mathbf{l}_j - \mathbf{l}_i)] [\mathbf{l}_j \cdot (\mathbf{l}_j - \mathbf{l}_i)] C_{l_i}^{\phi s} C_{l_j}^{\phi s} C_{|\mathbf{l}_j - \mathbf{l}_i|}^{\Theta} \\
& - 2 [\mathbf{l}_i \cdot (\mathbf{l}_i + \mathbf{l}_j)] [\mathbf{l}_j \cdot (\mathbf{l}_i + \mathbf{l}_j)] C_{l_i}^{\phi s} C_{l_j}^{\phi s} C_{|\mathbf{l}_i + \mathbf{l}_j|}^{\Theta}
\end{aligned} \tag{43}$$

V. RESULTS

In Fig 3, we show the scaled trispectra, where

$$\Delta_{\text{sq}}^{\Theta}(l) = \frac{l^2}{2\pi} T^{\Theta}(\mathbf{l}_i, -\mathbf{l}_i, \mathbf{l}_\perp, -\mathbf{l}_\perp)^{1/3}. \tag{44}$$

and $l_\perp = l$ and $\mathbf{l} \cdot \mathbf{l}_\perp = 0$. In the case of lensing alone, the trispectrum is proportional to square of the CMB anisotropy power spectrum (see, equation 35) and the sharp reduction in power at multipoles greater than a few thousand is effectively due to the decrease in primary anisotropy power at small angular scales. In the case of lensing-secondary correlation, the trispectrum is only proportional to one power of the CMB anisotropy power spectrum. Thus, the trispectrum now depicts more of the behavior of lensing-secondary correlation power spectrum shown in figure 2. The sharp decrease in the lensing-ISW trispectrum compared to that of the lensing-SZ effect is due to differences in the small angular scale power associated with lensing-ISW and lensing-SZ correlations.

We can now use this trispectrum to study the contributions to the covariance. In Fig. 4, we show the ratio of the diagonal of the full covariance to the Gaussian variance with the non-Gaussian term neglected:

$$R \equiv \frac{C_{ii}}{C_i}, \tag{45}$$

and for bands l_i given in Table I. Here, we have used rather wide bins in multipoles such that bin width is constant in logarithmic intervals in multipole space. This is the same binning scheme used by [26] on $6^\circ \times 6^\circ$ fields to investigate weak lensing covariance and later adopted by [11]. The two lines show the ratio when trispectra due to lensing and lensing-SZ correlations are used to calculate the covariance, respectively. The square root of the ratio is roughly the fractional change induced in errors along the diagonal resulting from the non-Gaussian covariance contributions. We do not show the ratio due to lensing-ISW trispectrum as the resulting changes are less than 10^{-6} at all multipoles of interest. As shown in figure 4, the ratio is less than 20% for weak lensing and peaks at multipoles ~ 4000 while the ratio increases to smallest scale with the lensing-SZ trispectrum.

The correlation between the bands is given by

$$\hat{C}_{ij} \equiv \frac{C_{ij}}{\sqrt{C_{ii}C_{jj}}}. \tag{46}$$

In Table I we tabulate the correlation coefficients for the CMB binned power spectrum measurements. The upper triangle here is the correlations under the lensing trispectrum while the lower triangle shows the correlations found with the trispectrum due to lensing-SZ correlations. In the case of lensing contribution to the tripsecrum, correlations depict the general shape of the CMB power spectrum while in the case of lensing-SZ contribution to the covariance, the correlation coefficients are more consistent with the shape of the lensing-SZ power spectrum.

In Fig. 5, we show the correlation coefficients for (a) lensing and (b) lensing-SZ contributions to the covariance. Here we show the behavior of the correlation coefficient between a fixed l_j (as noted in the figure) as a function of l_i . Note that when $l_i = l_j$ the coefficient is 1 by definition; we have not included this point in the figure due to the apparent discontinuity it creates from the the dominant Gaussian contribution at $l_i = l_j$.

To better understand how the non-Gaussian contribution scale with our assumptions, we consider the ratio of non-Gaussian variance to the Gaussian variance (see, [10,11])

$$\frac{C_{ii}}{C_i^G} = 1 + R, \tag{47}$$

with

$$R \equiv \frac{A_{si} T_{ii}^{\Theta}}{(2\pi)^2 2C_i^2}. \tag{48}$$

In the case of lensing alone contribution to CMB trispectrum, we can simplify the expression for R by noting that

$$T^{\Theta}(\mathbf{l}_i, -\mathbf{l}_i, \mathbf{l}_j, -\mathbf{l}_j)|_{l_i=l_j} \sim 8C_{l_i}^{\Theta} C_{l_i}^{\Theta} C_{\sqrt{2}l_i}^{\phi\phi} l_i^4 \tag{49}$$

where for an approximation we have taken $\mathbf{l}_i \cdot \mathbf{l}_j = 0$. Replacing the averaging of the product of $(C_{l_i}^{\Theta})^2 C_{l_i}^{\phi\phi}$ with the product of two averages, we can simplify the ratio of T_{ii}^{Θ}/C_i^2 to obtain

$$R \sim 4l_i \delta l_i \left\langle \frac{l_i^4 C_{l_i}^{\phi\phi}}{2\pi} \right\rangle_{A_i} \tag{50}$$

where $\langle \dots \rangle_{A_i}$ represents the averaging of the lensing potential powerspectrum, weighted by a factor of l_i^4 to represent the deflection angles. The equation (50) represents the general behavior of the non-Gaussian contribution to the lensing trispectrum. The relative contribution from non-Gaussianities scale with several parameters: (a) increasing the bin size, through δl_i ($\propto A_{si}$), leads to an increase in the non-Gaussian contribution linearly while (b) the contribution is determined by the shape of the

lensing potential power spectrum. At large multipoles, when $C_{l_i}^{\phi\phi}$ is a rapidly decreasing function, there is no significant contribution to the trispectrum and thus to the covariance. This is contrary to the general assumption that lensing is a small scale phenomena and that small-scale signal in CMB should be strongly affected by the non-linear nature of weak lensing. In the case of CMB, however, lensing effect is a large scale phenomena, especially given the power spectrum of lensing deflection angles peak at multipoles of ~ 40 and most of the lensing power is concentrated at degree angular scales instead of arcsecond scales.

For upcoming wide-field experiments, especially those involving satellite missions such as MAP and Planck, we do not expect non-Gaussianities to limit the interpretation and the cosmological parameter extraction from the measured CMB power spectrum. For these wide-field experiments, the width of the bin in multipole space will be of order at most few tens; for such small bin widths in multipole space at $l \sim$ few hundred will lead to a significantly reduced ratio of non-Gaussian to Gaussian contribution from what we have considered where $\delta l \sim l$. Also, note that the cosmologically interesting acoustic peak structure and the damping tail of the CMB anisotropies is limited to multipoles below ~ 1000 . In this range, there is no significant non-Gaussian contribution related to lensing and lensing-secondary correlations. There are, however, ground-based experiments (e.g., Cosmic Background Imager [28]) for which the non-Gaussianities due to lensing may be important. These small angular scale experiments, which probe the anisotropy power between multipoles of ~ 1000 and 4000 or so are likely to be limited to small areas on the sky and will utilize wide bins in multipole space when estimating the power spectrum in order to increase the signal-to-noise associated with its measurement. In such a scenario, it may be necessary to fully account for the full covariance when interpreting the power spectrum at small angular scales.

VI. SUMMARY

The upcoming small angular scale CMB anisotropy experiments are expected to provide first measurements of the power spectrum related to the damping tail and secondary anisotropies. At such scales, important non-linear effects and secondary contributions can imprint non-Gaussian signals on the CMB temperature fluctuations. Here, we discussed one aspect related to the presence of non-Gaussianities when measuring the CMB anisotropy power spectrum involving a contribution to the covariance resulting from the higher order four-point correlation function, or a trispectrum in Fourier space. Here, we discussed the non-Gaussian contribution to the power spectrum covariance of CMB anisotropies resulting through weak gravitational lensing angular deflections and the correlation of deflections with the integrated

Sachs-Wolfe effect and the Sunyaev-Zel'dovich effect.

With substantially wide bins in multipole space, the resulting non-Gaussian contribution from lensing to the binned power spectrum variance is insignificant out to multipoles of few thousand containing acoustic peaks and the damping tail, which are of substantial interest for cosmological parameter estimation purposes. For upcoming satellite based near all-sky experiments, we do not expect non-Gaussianities to limit the cosmological parameter extraction from CMB power spectrum measurements and their interpretation. For small angular scale ground-based experiments with substantially limited sky coverage, however, the presence of non-Gaussianities should be accounted when interpreting any measurements at angular scales corresponding to few arcminutes or multipoles ~ 4000 . Observational results related to this part of the CMB power spectrum is expected from a wide-variety of experiments based on interferometric and bolometric techniques.

ACKNOWLEDGMENTS

We acknowledge support from the Sherman Fairchild Foundation and from the DOE grant number D.E.-FG03-92-ER40701.

- [1] L. Knox, Phys. Rev. D, **52** 4307 (1995); G. Jungman, M. Kamionkowski, A. Kosowsky and D.N. Spergel, Phys. Rev. D, **54** 1332 (1995); J.R. Bond, G. Efstathiou and M. Tegmark, MNRAS, **291** L33 (1997); M. Zaldarriaga, D.N. Spergel and U. Seljak, Astrophys. J., **488** 1 (1997); D.J. Eisenstein, W. Hu and M. Tegmark, Astrophys. J., **518** 2 (1999)
- [2] E. Komatsu and D. N. Spergel, Phys. Rev. D, **63** 063002 (2001); L. Wang and M. Kamionkowski, Phys. Rev. D, 61, 063504 (1999); A. Gangui and J. Martin, MNRAS, 313, 323 (2000); X. Luo and D. N. Schramm, Phys. Rev. Lett., 71, 1124 (1994); X. Luo Astrophys. J., 427, 71 (1994); T. Falk, R. Rangarajan and M. Frednicki, Astrophys. J. Lett. 403, L1 (1993);
- [3] R. A. Sunyaev and Ya. B. Zel'dovich, MNRAS, **190**, 413 (1980);
- [4] D. N. Spergel and D. M. Goldberg, Phys. Rev. D**59**, 103001 (1999); D. M. Goldberg and D. N. Spergel, Phys. Rev. D, **59**, 103002 (1999); M. Zaldarriaga and U. Seljak, Phys. Rev. D, **59**, 123507 (1999); H. V. Peiris and D. N. Spergel, Astrophys. J., **540**, 605 (2000).
- [5] A. Cooray and W. Hu, Astrophys. J., **534**, 533 (2000).
- [6] A. Cooray, Phys. Rev. D, **64**, 043516 (2001)
- [7] A. Cooray, W. Hu and M. Tegmark, Astrophys. J., **540**, 1 (2000).
- [8] W. Hu, Phys. Rev. D, **62**, 043007 (2000).
- [9] M. Zaldarriaga, Phys. Rev. D, **62**, 063510 (2000).

ℓ_{bin}	529	739	1031	1440	2012	2812	3930	5492	7674
529	1.000	0.002	0.002	0.003	0.005	0.013	0.059	0.239	0.554
739	(0.000)	1.000	0.010	0.007	0.009	0.021	0.091	0.348	0.783
1031	(0.000)	(0.000)	1.000	0.013	0.012	0.025	0.090	0.318	0.686
1440	(0.000)	(0.000)	(0.000)	1.000	0.025	0.034	0.093	0.277	0.547
2012	(0.000)	(0.000)	(0.000)	(0.000)	1.000	0.060	0.092	0.200	0.336
2812	(0.000)	(0.000)	(0.000)	(0.000)	(0.000)	1.000	0.101	0.102	0.125
3930	(0.000)	(0.000)	(0.000)	(0.000)	(-0.001)	(-0.002)	1.000	0.039	0.021
5492	(0.000)	(0.001)	(0.000)	(0.000)	(-0.001)	(-0.005)	(-0.031)	1.000	0.001
7674	(0.000)	(0.001)	(0.000)	(0.000)	(0.000)	(-0.001)	(-0.016)	(-0.186)	1.000

TABLE I. Weak Lensing Convergence Power Spectrum Correlations. Upper triangle displays the covariance with the lensing trispectrum alone, while the lower triangle (parenthetical numbers) displays the covariance with the trispectrum due to lensing-SZ correlation. We do not tabulate the covariance due to trispectrum resulting from lensing-ISW correlation as the correlation coefficients are of order 10^{-6} or below. The data are binned such that bin sizes are constant in logarithmic intervals.

- [10] R. Scoccimarro, M. Zaldarriaga and L. Hui, *Astrophys. J.*, **527**, 1 (1999); D. J. Eisenstein and M. Zaldarriaga, *Astrophys. J.*, **546**, 2 (2001).
- [11] A. Cooray and W. Hu, *Astrophys. J.*, **554**, 56 (2001).
- [12] R. K. Sachs and A. M. Wolfe, *Astrophys. J.*, **147**, 73 (1967).
- [13] J. E. Carlstrom, M. Joy and L. Grego, *Astrophys. J.*, **456**, L75 (1996); M. Jones, R. Saunders, P. Alexander et al., *Nature*, **365**, 320 (1993).
- [14] A. Cooray, *Phys. Rev. D*, **64**, 063514 (2001).
- [15] N. Kaiser, *Astrophys. J.*, **388**, 286 (1992); N. Kaiser, *Astrophys. J.*, **498**, 26 (1998); M. Bartelmann & P. Schneider, *Physics Reports* in press, *astro-ph/9912508* (2000).
- [16] D. Limber, *Astrophys. J.*, **119**, 655 (1954).
- [17] P. J. E. Peebles, *The Large-Scale Structure of the Universe*, Princeton: Princeton Univ. Press (1980).
- [18] D. J. Eisenstein & W. Hu, *Astrophys. J.*, **511**, 5 (1999).
- [19] E. F. Bunn & M. White, *Astrophys. J.*, **480**, 6 (1997).
- [20] P. T. P. Viana & A. R. Liddle, *MNRAS*, **303**, 535 (1999).
- [21] W. Hu & M. White, *A&A*, **315**, 33 (1996).
- [22] U. Seljak & M. Zaldarriaga, *Phys. Rev. D*, **60**, 043504 (1999).
- [23] A. Cooray, *Phys. Rev. D*, **62**, 103506 (2000).
- [24] U. Seljak, *Phys. Rev. D*, submitted, *astro-ph/0001493* (2000); C.-P. Ma and J. N. Fry, *Astrophys. J.*, **538**, L107 (2000); R. Scoccimarro, R. Sheth, L. Hui and B. Jain, *Astrophys. J.*, **546** 20 (2001). A. Cooray, W. Hu and J. Miralda-Escude, *Astrophys. J. bf* 536, L9 (2000).
- [25] U. Seljak & M. Zaldarriaga, *Astrophys. J.*, **469**, 437 (1996).
- [26] White, M., Hu, W. 1999, *ApJ*, 537, 1
- [27] U. Seljak and M. Zaldarriaga, *Astrophys. J.*, **538**, 57 (2000).
- [28] S. Padin, M. C. Shepherd, J. K. Cartwright et al. preprint (*astro-ph/0110124*) (2001)